ACTA IMEKO
ISSN: 2221-870X
June 2025, Volume 14, Number 2, 1 - 9

Experimental analysis of blood pressure estimation using electrocardiography and photoplethysmography signals from fingertip measurements

Oleksandr Vasilevskyi[1], Roman Trishch[2], Volodymyr Sarana[3], Maksym Yakovlev[4], Emanuel Popovici[3]

[1] *The Walker Department of Mechanical Engineering, The University of Texas at Austin, 204 E Dean Keeton Street, Austin, TX 78712, USA*
[2] *Ukraine National Aerospace University "Kharkiv Aviation Institute", Kharkiv, Ukraine*
[3] *University College Cork, Cork. College Rd., T12 K8AF, Ireland*
[4] *Central Scientific Research Institute of Armament and Military Equipment of Armed forces of Ukraine, Kyiv, Ukraine*

ABSTRACT
This study investigates the indirect estimation of systolic and diastolic blood pressure using electrocardiography and photoplethysmography signals acquired from the fingertip. Two distinct approaches for blood pressure calculation were evaluated: one based on linear and non-linear models, and another utilizing mathematical models to determine diastolic pressure through mean arterial pressure. The research was conducted using the MAX86150 Evaluation System, with algorithm development and analysis performed in MATLAB. Blood pressure calculations were applied to two patients of different ages, and the results were compared. Additionally, the study examined measurement uncertainty and the role of statistical methods in data validation. It was established that the expanded measurement uncertainty does not exceed ± 11.55 mmHg for systolic blood pressure and ± 7.84 mmHg for diastolic blood pressure at a 95 % confidence level, which complies with the clinical accuracy requirements of the British Hypertension Society and the Association for the Advancement of Medical Instrumentation (AAMI/ANSI/ISO 81060-2:2018). The results showed that the approach based on the mathematical model of mean diastolic pressure demonstrated higher accuracy of arterial pressure estimation. The proposed algorithm exhibited strong reliability, highlighting the need for further validation against reference measurement tools in future research. However, a key limitation of the study is the small sample size — measurements were conducted on only two patients, which significantly restricts the generalizability of the findings.

Section: RESEARCH PAPER

Keywords: Indirect blood pressure measurement; ECG and PPG signals; digital stethoscope; systolic pressure; diastolic pressure

Citation: O. Vasilevskyi, R. Trishch, V. Sarana, M. Yakovlev, E. Popovici, Experimental analysis of blood pressure estimation using electrocardiography and photoplethysmography signals from fingertip measurements, Acta IMEKO, vol. 14 (2025) no. 2, pp. 1-9. DOI: 10.21014/actaimeko.v14i2.2096

Section Editor: Elisabeth Costa Monteiro, Pontifical Catholic University of Rio de Janeiro, Brazil

Received March 31, 2025; **In final form** June 16, 2025; **Published** June 2025

Corresponding author: Oleksandr Vasilevskyi, e-mail: oleksandr.vasilevskyi@austin.utexas.edu

1. INTRODUCTION

Accurate estimation of blood pressure (BP) remains a persistent challenge in both clinical and everyday settings. While conventional cuff-based methods provide reliable measurements, they are unsuitable for continuous or wearable applications. In response to this limitation, numerous studies have explored cuffless BP estimation techniques using physiological signals, particularly the electrocardiography (ECG) and photoplethysmography (PPG) [1]–[5]. These approaches employ different devices, sensors, and mathematical models to estimate systolic and diastolic pressure [1], [2], [6], yet their accuracy and reliability vary significantly.

The motivation behind this study is to develop a compact, low-complexity algorithm for estimating systolic blood pressure (SBP) and diastolic blood pressure (DBP) using only ECG and PPG signals recorded from the fingers. The proposed method is specifically designed for integration into a small-diameter (50 mm) electronic stethoscope [7]–[9], enabling seamless deployment in portable medical devices for enhancing its diagnostic capabilities. Unlike many existing approaches, this work not only introduces a new modelling framework but also provides a complete measurement uncertainty analysis. This analysis includes both Type A (statistical) and Type B (instrumental and methodological) evaluation of uncertainties,

allowing for a more rigorous evaluation of the system's accuracy and comparability with laboratory standards.

The main contributions of this study are:

- The development and comparison of two mathematical models for SBP and DBP estimation using finger-based ECG and PPG signals.
- Implementation of the algorithm in MATLAB for integration into a stethoscope-based monitoring system.
- A methodology for evaluating measurement uncertainty, addressing a critical gap in most existing studies.

2. RELATED WORKS

Numerous studies have examined methods for non-invasive BP estimation using combinations of physiological signals, machine learning algorithms, and pulse wave analysis. Below is an overview of key contributions and their limitations.

Research by Paul C.-P. Chao et al. [1], focused on BP estimation using cuffless sensors, demonstrated a wide range of methods and algorithms for accurate estimation of SBP and DBP. Traditional methods, based on the analysis of ECG and PPG signals, face certain limitations in accuracy and computational complexity due to the dynamic nature of the human cardiovascular system. However, methods using pulse wave velocity (PWV), such as the Bramwell-Hill equation, have shown potential in theoretical BP calculation models. The application of methods such as pulse transit time (PTT) or pulse arrival time (PAT) has improved the accuracy of SBP and DBP prediction, but the dynamic nature of the human body in real conditions complicates accurate forecasting. Despite the successes, many of the algorithms proposed by the authors exhibit large errors, particularly in predicting DBP. They suggested using algorithms such as adaptive boosting (AdaBoost) and deep recurrent neural networks (BiLSTM), which allowed for more accurate long-term results; however, the high computational complexity of these models limits their practical application. It is important to note that most studies used pre-defined features of the signals, which also impacts the accuracy of the final models. Machine learning systems, such as deep neural networks and supervised learning methods, have shown significant improvements in BP prediction accuracy, but they remain sensitive to feature selection, training data, and the number of processed samples. The main challenges are the need for calibration, physiological dependencies' complexity, and models' high computational complexity. Despite these advances, further improvements in BP prediction require the development of new algorithms that will account for greater variability in physiological factors and optimize computational resources to ensure real-time accuracy.

Yan J. et al. [2] in this study effectively use the fusion of ECG, PPG, and PPW signals along with the Random Forest Regression (RFR) algorithm for predicting BP. The results indicate that demographic factors and physiological signal features such as PWV-a, ECG, and PPW significantly contribute to predicting both SBP and DBP. However, the study faces limitations, including a lack of sample diversity and challenges in applying the approach for long-term monitoring. In this study, the RFR model demonstrated superior performance for predicting SBP and DBP. The Mean Absolute Error (MAE) for SBP prediction was 0.90 mmHg, and for DBP, it was 0.64 mmHg. The standard deviation (STD) was 2.47 mmHg for SBP and 1.53 mmHg for DBP. The feature fusion method notably improved prediction performance, outperforming other algorithms like Gaussian Process Regression and Support Vector Machine. However, the considered method has the following significant drawbacks: the selection of optimal features using RFR and Sequential Forward Selection may require large computational resources and large datasets to avoid overfitting; the model may be less reliable for populations not included in the study group (e.g., individuals without cardiovascular diseases); implementing this model in real-time systems may be challenging due to the computational requirements.

The study by Yan et al. [3] demonstrates the transferability of ECG-based foundational models for estimating BP using ECG and PPG signals. By fine-tuning a pre-trained transformer model on ECG/PPG data, the method achieves near-state-of-the-art performance for both DBP and SBP with minimal computational overhead. The results show a MAE of 1.57 mmHg for DBP and 2.72 mmHg for SBP. Additionally, dynamic Integer 8-bit (INT8) quantization reduced the model size significantly, making it suitable for resource-constrained devices. The approach promises unobtrusive, continuous BP monitoring for both clinical and home use. However, the work [3] focuses exclusively on a machine learning algorithm for modelling signals based on ECG and PPG monitoring, utilizing a variable attention mechanism to reduce memory requirements. The study does not describe a method for calculating BP values from the measured ECG and PPG signals. Furthermore, work [3] is aimed at continuous ECG and PPG signal monitoring, whereas our proposed approach is intended for instantaneous BP measurement, enabling integration into portable medical devices (an electronic stethoscope). In addition, work [3] lacks a methodology for evaluating measurement uncertainty, which significantly limits the ability to compare the obtained results with those from other laboratories.

The study [4] highlights the challenges of using PWV for BP estimation. Methods such as PAT and PTT are central, but they require accurate timing of events like the aortic valve opening. Alternative methods like seismocardiography (SCG) and gyrocardiography (GCG) aim to bypass the complexities of the pulse ejection period (PEP). Remote PPG has emerged as a contactless solution, offering portability and ease of use for continuous BP monitoring.

The study by Samimi and Dajani [5] presents an innovative cuffless BP estimation method based on the analysis of PPG, opening new possibilities for continuous and non-invasive cardiovascular monitoring. The method relies on the estimation of reflected pulse transit time (R-PTT) derived from PPG signals recorded from peripheral blood vessels. To enhance accuracy, the authors employ a calibration model based on the Moens-Korteweg and Bramwell-Hill equations, allowing for the consideration of individual arterial properties, including elasticity. Machine learning algorithms, particularly artificial neural networks, are utilized for data processing and prediction of SBP and DBP values.

Despite the high correlation between the predicted and measured BP values, the proposed method has several limitations. First, its accuracy is highly dependent on the quality of the initial PPG signals, which can be distorted due to patient movement, changes in peripheral blood flow, and artifacts caused by external factors. Second, the method requires prior calibration using conventional BP measurements, reducing its autonomy and universal applicability. Additionally, individual physiological characteristics, such as vascular tone, hydration levels, and overall cardiovascular condition, can introduce variability, necessitating further research to improve the model's

adaptability. The authors emphasize the need for more robust signal processing algorithms and optimized calibration methods to enhance the system's accuracy and reliability. Overall, the proposed approach represents a significant advancement in digital health technologies and holds great potential for widespread clinical application in the future.

The review by Sharma et al. [6] provides a comprehensive analysis of methodologies for cuffless and continuous BP monitoring, emphasizing the technological advancements and challenges in this field. The authors categorize existing approaches based on the physiological signals used, including PPG, ECG, PTT, and tonometry. They discuss various signal-processing techniques and machine learning algorithms employed to estimate BP non-invasively, highlighting their advantages and limitations. The study also examines the integration of wearable and IoT-based devices, showcasing their potential in real-time health monitoring. One of the key contributions of this review is its in-depth comparison of different methodologies in terms of accuracy, calibration requirements, and usability in clinical and consumer applications. The authors highlight that while PTT-based methods show promise, they require individual calibration and are sensitive to physiological variations such as arterial stiffness and hydration levels. Machine learning models, although improving accuracy, often face challenges related to dataset generalization and model interpretability. Additionally, the review identifies key limitations, including sensor placement issues, motion artifacts, and environmental interferences that affect signal quality. Despite significant progress in cuffless BP monitoring, the review underscores the need for standardization in validation protocols, larger datasets for machine learning training, and improvements in sensor technology. The study serves as a valuable reference for researchers and engineers working on the development of next-generation BP monitoring systems, providing insights into current gaps and future directions for enhancing accuracy, reliability, and user-friendliness. PTT is strongly correlated with SBP and DBP but requires frequent individual calibration due to physiological variations like arterial compliance and hydration levels. Accuracy varies significantly, with MAEs ranging from 5 to 10 mmHg, depending on the calibration approach.

A review of existing BP measurement techniques revealed significant challenges, including high complexity, difficulties in practical implementation, and low accuracy and sensitivity across different age groups and BP ranges. Furthermore, inconsistencies in how researchers interpret and apply mathematical models for BP estimation contribute to variations in results. Differences in the equipment used also lead to waveform distortions that deviate from theoretical expectations described in the literature [1]-[5], [10].

To overcome these challenges and expand the functionality of the electronic stethoscope [7], we developed and tested an algorithm in MATLAB for indirect SBP and DBP estimation using ECG and PPG signals from the fingers. The proposed approach utilizes two distinct models for BP prediction, enabling a comparative evaluation of their accuracy and effectiveness.

Compared to the existing research, the novelty of this work lies in the development and detailed description of mathematical models that enable accurate calculation of SBP and DBP values based on ECG and PPG signals. Furthermore, this study is the first to present a methodology for evaluating BP measurement uncertainty that accounts for Type A evaluation of uncertainty, Type B evaluation of uncertainty associated with the limited accuracy of the measuring equipment, and the combined and expanded uncertainties.

Figure 1. The MAX86150 Evaluation System used for ECG and PPG signal measurements.

3. EQUIPMENT AND MEASUREMENT MODEL

3.1. System for measuring ECG and PPG signals

For the experiments, we utilized the MAX86150 Evaluation System (Figure 1), a validated platform designed for assessing the MAX86150 integrated PPG and single-lead ECG sensor module [11]. The system comprises two interconnected boards: the MAX32630FTHR microcontroller board and the MAX86150 evaluation kit, connected via header pins. The MAX32630FTHR board features a microcontroller with preloaded firmware, Bluetooth communication, and power management, while the sensor board houses the MAX86150 module along with two stainless steel dry electrodes for ECG acquisition. The system operates on a lithium-ion battery, rechargeable via a micro-USB cable [11].

Using this evaluation system, we conducted ECG and PPG signal measurements exclusively from the fingers. The data collection was performed on patients of different ages (42 years old - Patient 1, 66 years old - Patient 2). The recorded measurement results were stored in CSV files and subsequently processed using the proposed algorithm in MATLAB to estimate the patients' SBP and DBP values.

The ECG channel is designed with a differential input range of ± 1.3 V (typically 1.8 V), ensuring accurate capture of the heart's electrical signals. The PPG channel supports up to 6 LEDs and 4 photodiode inputs, offering flexibility in adapting to various measurement conditions. The system provides a resolution of 18 bits for ECG signals with a sampling rate of 230 Hz (with a bandwidth of 0.05 Hz – 40 Hz) and achieves a common-mode rejection ratio (CMRR) of over 110 dB at 50 Hz and 60 Hz, ensuring high accuracy in capturing heart signals. For PPG signals, the system offers a resolution of 19 bits, with a noise suppression level of 90 dB at 120 Hz, enabling clean and stable signal acquisition. The system operates with an energy-efficient power consumption of approximately 1.15 mA per channel, making it ideal for continuous monitoring, and is designed to function within a temperature range of –40 °C to +85 °C. These characteristics make the MAX86150 system a highly effective solution for portable and precise health monitoring applications, providing high-quality ECG and PPG signal recording.

Under ideal conditions - such as stable skin contact and minimal motion - the PPG sensor provides heart rate measurements with an accuracy of ± 3 beats per minute (bpm), which corresponds to a relative accuracy of $\gamma_1 = 4.3$ % assuming a typical resting heart rate of 70 bpm. The relative accuracy of the ECG channel is estimated at $\gamma_2 = 0.08$ %, derived from a

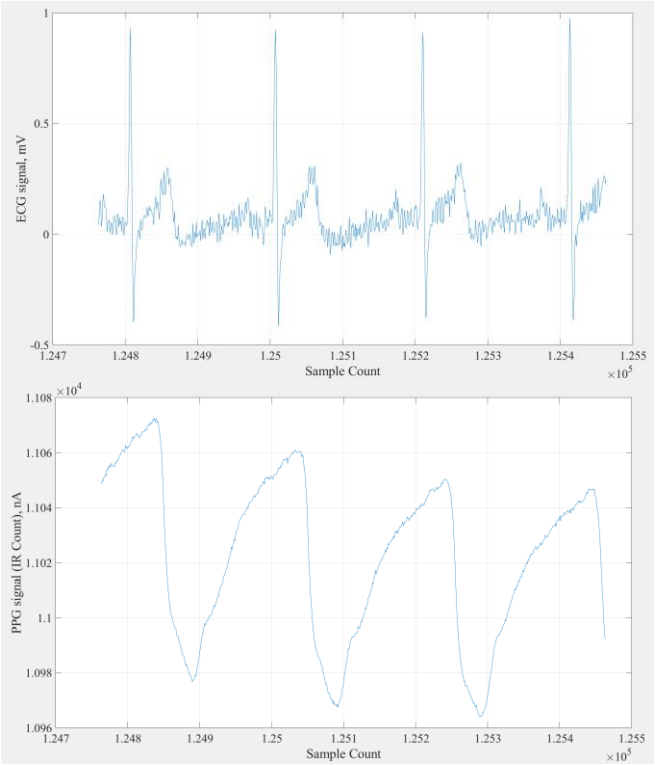

a)

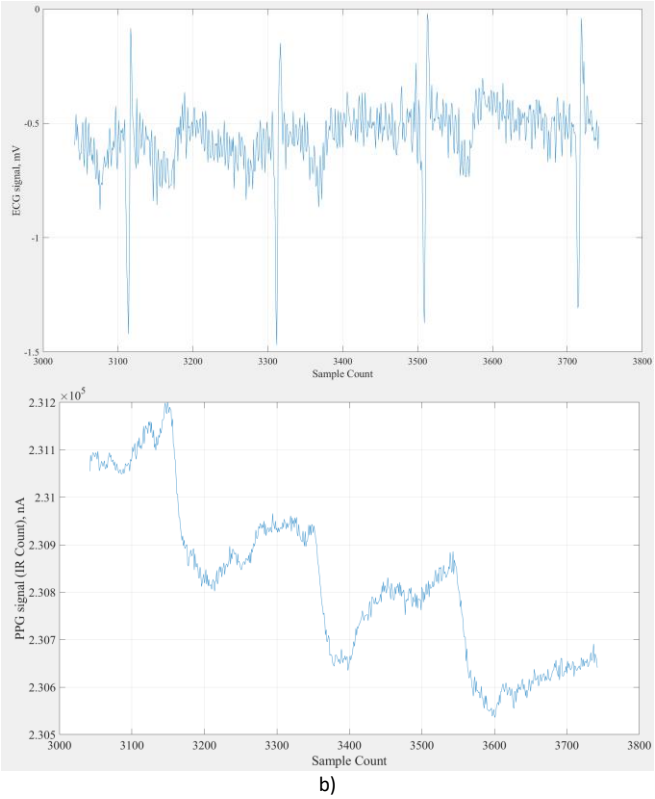

b)

Figure 2. Illustration of a typical waveform of the PPG and ECG: a) ECG and PPG signals of patient 1; b) ECG and PPG signals of patient 2.

typical input-referred noise of approximately 1.2 μV and a typical resting ECG signal amplitude of approximately 1.5 mV observed in healthy individuals [11].

Thus, the MAX86150 Evaluation Board demonstrates relative measurement accuracy typically under 5 %, making it suitable for research-grade physiological signal monitoring. Final accuracy depends on signal processing algorithms, environmental conditions, and application-specific calibration.

3.2. Methodology for processing measured ECG and PPG signals

Using the MAX86150 Evaluation System described above, multiple measurements of ECG and PPG signals were performed on two healthy patients of different ages. As a result of long-term ECG and PPG signal measurements taken from the fingers, a database was created, with signal segments from this data shown in Figure 2.

Figure 2a and Figure 2b present multiple periods of ECG and PPG signals recorded from two patients. A maximum search function was applied to these signals. To provide a clear and detailed explanation of the methodology for determining SBP and DBP, we have selected a single period of the ECG and PPG signals, as shown in Figure 3.

Figure 2 and Figure 3 demonstrate that the PPG signals obtained with the MAX86150 Evaluation System exhibit a slightly different (inverse) waveform compared to those reported in the literature [1], [5], [12]. This discrepancy may be attributed to variations in the equipment and software used for measuring ECG and PPG signals.

To determine the pulse transit time interval, which characterizes the systolic pressure PTT, we calculated the difference between the t_2 interval and the t_1 interval:

$$PPT = t_2 - t_1. \quad (1)$$

At the same time, the t_2 interval was defined as the difference between the ECG signal peak and the PPG signal minimum, and the t_1 interval was defined as the difference between the ECG signal peak and the PPG signal maximum (Figure 3).

The number of samples corresponding to the PTT interval between the extrema of the ECG and PPG signals was then converted into time ts (time between the PPG peak and the PPG

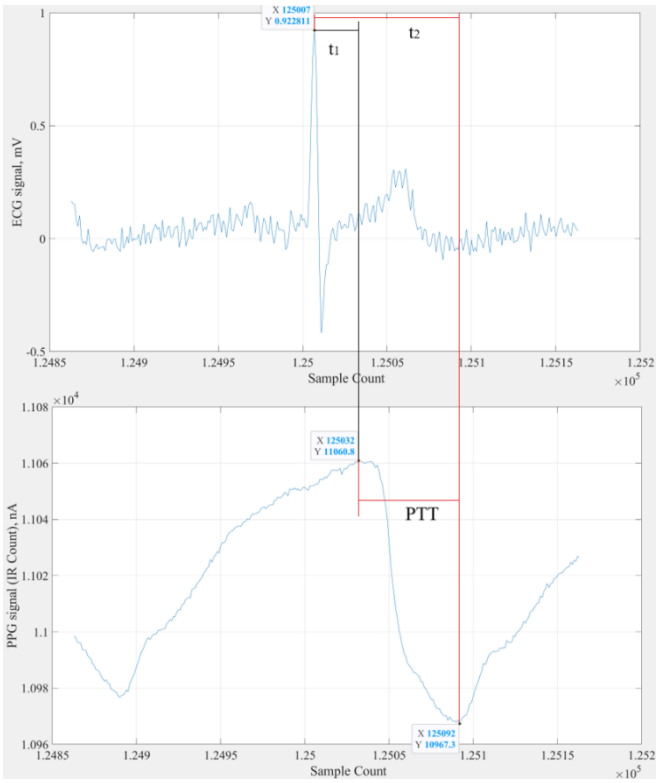

Figure 3. Demonstration of the methodology for determining SBP and DBP parameters based on PTT calculation from the ECG and PPG signals.

foot point (diastolic minimum, ms), considering the sampling rate of 200 kHz, using the following formula:

$$ts = (PPT/200) \cdot 1000. \quad (2)$$

It is important to note that ts alone is not a direct measure of BP. Its reliability as a BP indicator depends on several physiological and measurement factors, including heart rate variability, vascular tone, and measurement site. Therefore, in our approach, ts is used not as a standalone predictor but as one of the parameters incorporated into a broader mathematical model that also includes additional signal features to improve robustness and accuracy of the indirect BP estimation.

Considering the aforementioned formulas (1) and (2), along with the recommendations from previous studies [6], [9], [12], [13], we calculated the SBP using two different equations:

$$SBP_1 = a_1 \cdot ts + b_1 \quad (3)$$

$$SBP_2 = a_2/t_2 + b_2. \quad (4)$$

The DBP for both patients was calculated using two different equations [9]:

$$DBP_1 = a_1 \cdot t_1 + b_1 \quad (5)$$

$$DBP_2 = a_2/t_1 + b_2. \quad (6)$$

A wide range of mathematical models for indirectly estimating BP from ECG and PPG signals is presented in [14]. These models utilize various types of equations, including linear, quadratic, and exponential, each derived from different theoretical approaches. For instance, equation (4) illustrates the inverse correlation between PTT and SBP, as demonstrated in numerous studies. This relationship is based on the principle that an increase in SBP shortens the time required for the pressure pulse to travel from proximal to distal sites, and vice versa [14], [15]. Through a comprehensive analysis and experimental validation of different equation types, and considering the recommendations of previous researchers [6], [12]–[15], we selected two specific models for indirect BP estimation, represented by equations (3)–(6). Other equation types showed either low sensitivity to BP variations or did not significantly improve the accuracy of SBP and DBP estimation.

3.2.1. Linear Method for SBP and DBP Estimation.

In the first approach for BP estimation (SBP_1 and DBP_1), linear mathematical models described by Equations (3) and (5) were employed. In this method, SBP, Equation (3), was calculated using the PTT interval between the extrema of the PPG signal, specifically the time ts between the PPG peak and the PPG diastolic minimum (Figure 3). For DBP estimation, Equation (5), the time interval t_1 between the peak points of the ECG and PPG signals was used. The constant coefficients a_1 and b_1 were assigned the numerical values previously calculated and justified in studies [9], [13]-[17]. These coefficients are set to a_1 = -0.5 and b_1 = 164 for the determination of SBP_1 in model (3), and a_1 = -0.5 and b_1 = 125 for the determination of DBP_1 in model (5). After applying this method based on the linear models (3) and (5) to the measured ECG and PPG signal parameters of two patients, the resulting BP estimations were obtained and are presented in Section 4, Table 1 (Method 1).

3.2.2. Nonlinear Method for SBP and DBP Estimation.

The second method is based on the use of nonlinear mathematical models (4) and (6). In this approach, SBP (4) is determined using the time interval t_2 between the ECG peak and the diastolic minimum of the PPG signal (Figure 3). And DBP (6) is estimated using the time interval t_1 between the peaks of the ECG and PPG signals (Figure 3).

For the second method of BP estimation (SBP_2 and DBP_2), the coefficients a_2 and b_2 in equations (4) and (6) were determined by solving a system of equations (7). The calculations utilized experimentally obtained time interval values PTT_S = 640 ms for SBP and PTT_D = 140 ms for DBP (reference values) along with the application of standard BP values – SBP_{normal} = 120 mmHg and DBP_{normal} = 80 mmHg – recommended by the American Heart Association [18], [19]:

$$\begin{cases} SBP_{\text{normal}} = \dfrac{a_2}{PTT_S} + b_2; \\ DBP_{\text{normal}} = \dfrac{a_2}{PTT_D} + b_2. \end{cases} \quad (7)$$

By solving the system of equations (7) with the known normal pressure values, the numerical coefficients a_2 = - 7170.87 and b_2 = 131.22 were derived. These coefficients were then used to process the measured ECG and PPG signal from several healthy individuals of different ages, enabling the determination of BP using formulas (4) and (6) within the MATLAB environment. The BP measurement results based on the nonlinear models (4) and (6) are presented in Section 4, Table 1 (Method 2).

3.2.3. Linear Method Using Mean Blood Pressure (MBP) for DBP Estimation.

The third approach is based on the use of Mean Blood Pressure (MBP) as an intermediate parameter for estimating DBP. As established in previous studies [5], [20]–[22], MBP is a hemodynamic parameter defined as a function of SBP and DBP values and is typically calculated using equation (8):

$$MBP = \frac{SBP}{3} + 2 \cdot \frac{DBP}{3}. \quad (8)$$

Using the aforementioned normal (reference) BP values SBP_{normal} = 120 mmHg, and DBP_{normal} = 80 mmHg [18], [19], the corresponding normal (reference) value of MBP_{normal} can be determined. According to equation (8), it corresponds to the value: $MBP_{normal} = SBP_{normal}/3 + 2 \cdot DBP_{normal}/3$ = 93.33 mmHg.

In this approach, using the linear model (3) for the estimation of SBP, the DBP can be expressed in terms of the normal (reference) value of MBP_{normal} according to equation (9):

$$\begin{aligned} DBP_3 &= 1.5 \cdot \left[MBP_{\text{normal}} - \frac{SBP_1}{3}\right] \\ &= 1.5 \cdot \left[MBP_{\text{normal}} - \frac{a_1 \cdot ts + b_1}{3}\right]. \end{aligned} \quad (9)$$

Applying this third approach, which is based on the linear model (3) for estimating SBP and model (9) for estimating DBP, to the measured parameters of the ECG and PPG signals from two patients, the BP values were assessed. The numerical results are presented in Section 4, Table 2 (Method 3).

3.2.4. Nonlinear Method Using MBP for DBP Estimation.

In the fourth approach, a nonlinear mathematical model (10) was investigated for estimating SBP using the interval *ts* between the extrema (the peak and the diastolic minimum) of the PPG signal (Figure 3):

$$SBP_{\text{PPT3}} = a_2/ts + b_2. \quad (10)$$

Using the nonlinear model (10) for SBP estimation and the reference value of MBP_{normal}, an expression was derived for *DBP* estimation:

$$DBP_4 = 1.5 \cdot \left[MBP_{\text{normal}} - \frac{a_2/ts + b_2}{3}\right]. \quad (11)$$

As a result of applying the nonlinear models (10) and (11) for blood pressure estimation, the results obtained are presented in Section 4, Table 2 (Method 4).

Using mathematical models (1)-(11), experimental data were analysed to indirectly estimate SBP and DBP in two patients aged 42 and 66 years. All computations were performed in MATLAB, which was selected for its compatibility with the CSV-format data exported from the MAX86150 evaluation system and its robust capabilities for signal processing. Additionally, MATLAB is commonly used in this field, offering built-in functions for signal filtering and denoising [23], [24].

The MAX86150 evaluation system was employed as a cost-effective and ready-to-use solution for acquiring and storing ECG and PPG signals. However, the proposed blood pressure estimation algorithm is not limited to this hardware and can be applied to data from other systems capable of measuring ECG and PPG signals, making it adaptable to various technologies and measurement platforms.

4. RESULTS

Based on the mathematical models discussed in the previous section, experimental values of SBP and DBP were obtained from two patients of different ages. Table 1 presents the results

Table 1. Experimental data for BP determination in two individuals using linear (Method 1) and nonlinear (Method 2) methods.

Patient 1		Patient 2	
Method 1 (*SBP/DBP*, mmHg)	**Method 2 (*SBP/DBP*, mmHg)**	**Method 1 (*SBP/DBP*, mmHg)**	**Method 2 (*SBP/DBP*, mmHg)**
112.50/84.00	113.73/86.40	104.50/84.00	118.64/90.24
111.75/89.00	113.94/83.41	112.50/84.00	113.73/90.24
117.00/86.50	108.46/84.96	112.25/91.50	113.29/90.24
119.50/56.50	109.16/97.87	112.50/96.50	112.59/90.24
113.00/86.50	113.07/84.96	112.00/81.50	114.35/90.24
162.25/84.00	143.48/86.40	114.50/76.50	112.59/90.24
112.75/84.00	113.51/86.40	111.50/99.00	113.29/76.06
113.25/89.00	112.59/83.41	112.50/89.00	113.29/83.41
112.50/89.00	113.29/83.41	112.00/89.00	113.73/83.41
111.50/99.00	113.29/76.06	113.25/89.00	112.59/83.41
113.75/76.50	113.29/90.24	111.75/89.00	113.94/83.41
113.25/84.00	113.07/86.40	112.00/81.00	114.35/87.76
112.75/94.00	112.59/80.00	111.25/81.50	114.92/87.76
112.25/91.50	113.29/81.77	111.75/84.00	114.35/86.40
113.00/86.50	113.07/84.96	112.00/79.00	114.54/89.04
113.25/84.00	113.07/86.40	111.50/84.00	114.54/90.24
117.50/76.50	109.16/90.24	112.00/81.50	114.35/90.24
118.00/64.00	110.13/95.37	111.75/79.00	114.74/90.24
117.00/66.50	111.02/94.45	111.00/86.50	114.74/90.24
117.75/64.00	110.43/95.37	112.00/81.50	114.35/87.76
***Mean*, mmHg**		***Mean*, mmHg**	
116.70/81.75	**113.68/86.92**	**111.73/85.35**	**114.15/87.54**
u_A , mmHg		**u_A, mmHg**	
10.99/11.12	**7.22/5.54**	**1.86/5.84**	**1.29/3.82**

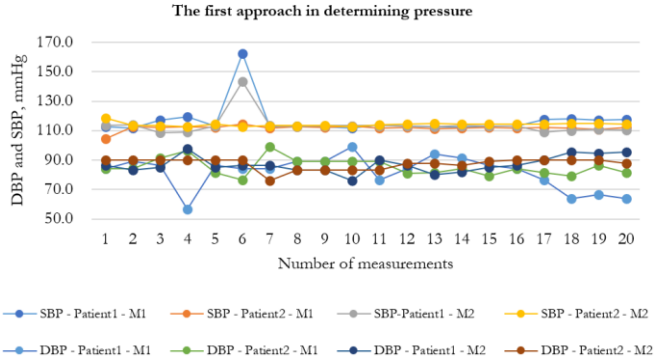

Figure 4. Variations in SBP and DBP in two patients of different ages.

of BP measurements derived using both the linear method (Subsection 3.2.1, Method 1) and the nonlinear method (Subsection 3.2.2, Method 2) for estimating SBP and DBP. The measurements for each subject were conducted in a seated resting state. For each subject, a series of 20 recordings of ECG and PPG signals were acquired under identical conditions. Each recording lasted approximately 20 seconds (with the sample consisting of more than 4200 records of signal amplitude values with a sampling rate of 200 kHz), during which the subject was instructed to remain still and avoid talking or moving to minimize motion artifacts. During this time interval, approximately 22 periods of the PPG and ECG signals were recorded in a single session for each patient.

In addition to the numerical values, Figure 4 illustrates the variations in SBP and DBP for both patients, as calculated using Method 1 (M1) and Method 2 (M2). The figure provides a graphical comparison of the pressure changes across different age groups, highlighting the differences in the results obtained from the ECG and PPG signals. These visual representations help to better understand how the two methods perform in practice, considering factors such as age and signal characteristics. The comparison also allows for an evaluation of the consistency and accuracy of each method in estimating BP.

The results of a study of two other linear (Subsection 3.2.3, Method 3) and non-linear (Subsection 3.2.4, Method 4) methods for determining BP based on determining DBP through MBP and SBP values are presented in Table 2. In Method 3 (Subsection 3.2.3), the linear expression (3) was used to determine SBP, while expression (9) was applied to determine DBP. In Method 4 (Subsection 3.2.4), SBP was estimated using the nonlinear expression (10), and DBP was calculated using expression (11).

Figure 5 illustrates the characteristics of changes in SBP and DBP in two patients of different ages, based on the use of MBP with linear (Method 3, M3) and nonlinear (Method 4, M4) methods for determining SBP.

The Type A evaluation of measurement uncertainty [25]-[29] for SBP and DBP was calculated based on the results of experimental studies using the following formula:

$$u_{\text{A}} = \left[\frac{\sum_i^n (BP_i - \overline{BP})^2}{n(n-1)}\right]^{0.5}. \quad (12)$$

This study presents the results of only 20 measurements, selected from a dataset of over 1000 BP readings. As shown in Equation (12), these 20 measurements were repeated 20 times to demonstrate the methodology for calculating measurement uncertainty.

Table 2. Experimental data for BP determination in two individuals using MBP, based on the linear SBP estimation method (Method 3) and the nonlinear SBP estimation method (Method 4).

Patient 1		Patient 2	
Method 3 (*SBP/DBP*, mmHg)	**Method 4 (*SBP/DBP*, mmHg)**	**Method 3 (*SBP/DBP*, mmHg)**	**Method 4 (*SBP/DBP*, mmHg)**
112.50/83.75	112.54/83.73	112.00/84.00	113.64/83.18
111.75/84.12	114.16/82.92	111.25/84.37	115.14/82.43
110.00/85.00	117.32/81.34	111.75/84.12	114.16/82.92
113.00/83.50	111.34/84.33	112.00/84.00	113.64/82.73
112.50/81.50	112.54/83.73	112.25/83.88	113.64/83.18
113.25/83.37	110.71/84.65	112.00/84.00	113.64/83.18
112.75/83.62	111.95/84.02	112.00/84.00	113.64/83.18
113.25/83.37	110.71/84.65	112.50/83.75	112.54/83.73
111.25/84.37	115.14/82.43	111.75/84.12	114.16/82.92
112.50/83.75	112.54/83.73	110.00/85.00	117.32/81.34
111.50/84.25	114.66/82.67	112.25/83.88	113.10/83.45
113.75/83.13	109.35/85.33	112.00/84.00	113.64/83.18
115.25/82.38	104.75/87.78	111.5/84.25	114.66/82.67
113.25/83.37	110.71/84.64	113.00/83.50	111.34/84.33
112.50/83.75	112.54/83.73	112.50/83.75	112.54/83.73
112.75/83.62	111.95/84.02	113.75/83.13	109.35/85.33
112.25/83.88	113.10/83.45	112.75/83.62	111.95/84.02
113.00/83.50	111.34/84.33	113.25/83.37	110.71/84.65
113.25/83.37	110.71/84.65	112.00/84.00	113.64/83.18
112.25/83.88	113.10/83.45	113.25/83.37	110.71/84.65
114.00/83.00	108.63/85.69	111.25/84.37	115.14/82.43
114.75/82.62	106.24/86.88	112.25/83.75	112.54/83.73
117.75/81.12	121.33/79.34	111.50/84.25	114.66/82.67
***Mean*, mmHg**		***Mean*, mmHg**	
113.00/83.40	**112.06/83.98**	**112.12/83.93**	**113.28/83.34**
u_A , mmHg		**u_A, mmHg**	
1.52/0.86	**3.39/1.71**	**0.79/0.40**	**1.72/0.87**

A comparison of the Type A evaluation of measurement uncertainties presented in Table 1 and Table 2, obtained using two different approaches for determining SBP and DBP, reveals that the deviations are significantly smaller when employing the second approach (Table 2). Specifically, SBP was determined through the values of ts (the number of readings between the maximum of the ECG and PPG signals), and DBP was derived accordingly, considering the normal MBP_{normal} value.

The results of the study indicate that when using the nonlinear BP estimation method (Method 2), based on models (4) and (6), the experimental standard deviation (type A evaluation of measurement uncertainty) was lower compared to the linear method (Method 1), which is based on models (3) and (5). The Type A evaluation of measurement uncertainty for the first patient was 7.22 mmHg for SBP and 5.54 mmHg for DBP, while for the second patient, it was 1.29 mmHg for SBP and 3.82 mmHg for DBP.

Methods 3 and 4 (Table 2), which are based on the use of the normal MBP value (8) for calculating DBP using SBP values determined by equation (3) for the linear transformation model and by equation (10) for the nonlinear transformation model, yielded the following experimental measurement uncertainties. When using Method 3, in which SBP was determined by equation (3) and DBP by equation (9), Patient 1 exhibited a higher experimental Type A evaluation of measurement uncertainty than Patient 2. The uncertainties reached 1.52 mmHg

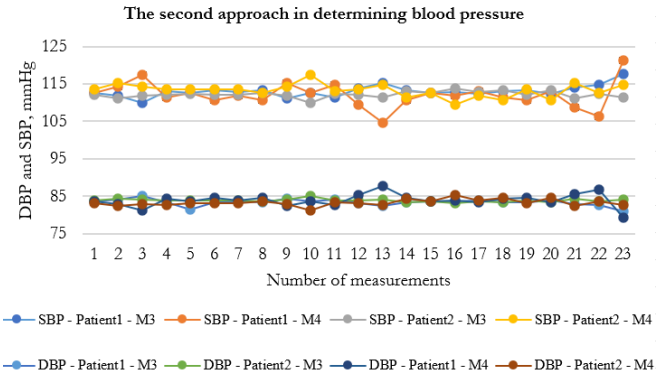

Figure 5. Characteristics of SBP and DBP changes in two patients of different ages based on MBP.

for SBP and did not exceed 0.86 mmHg for DBP, with an average BP of 113/83.4 mmHg. In Method 4, which applied the nonlinear transformation model (10) for SBP estimation and model (11) for DBP estimation, the maximum experimental measurement uncertainties were $u_{A_{SBP}} = 3.39$ mmHg for SBP and $u_{A_{DBP}} = 1.71$ mmHg for DBP, while the average BP ($\overline{BP}$) was 112/84 mmHg for Patient 1.

The obtained BP measurement results comply with the clinical accuracy requirements of the Association for the Advancement of Medical Instrumentation (AAMI/ANSI/ISO 81060-2:2018) standard. According to these guidelines, the Type A evaluation of uncertainty of MBP_{normal} (i.e., the standard deviation of the measurement error) must not exceed 8 mmHg.

To calculate the combined measurement uncertainty, which accounts for systematic effects related to the limited accuracy of the measurement system, the relative Type A evaluation of uncertainty was computed using the following formula:

$$\tilde{u}_A = \frac{u_A}{\overline{BP}} 100\ \%\,. \tag{13}$$

Substituting the corresponding values into Equation (13), the resulting relative Type A evaluation of uncertainty was 3.03 % for *SBP* and 2.04 % for *DBP*.

Considering the relative Type A evaluation of uncertainty and the accuracy specifications of the measurement channels (Type B evaluation of measurement uncertainties) as stated in the technical documentation - $\gamma_1 = 4.3$ % for the PPG channel and $\gamma_2 = 0.08$ % for the ECG channel - the relative combined measurement uncertainty was determined by Equation (14):

$$\tilde{u}_c = \left(\tilde{u}_A{}^2 + \gamma_1^2 + \gamma_2^2\right)^{0.5} \tag{14}$$

Thus, the relative combined measurement uncertainty of BP was 5.26 % for SBP and 4.76 % for DBP.

Using the coverage factor value $k_p = 1.96$ at a confidence level of $p = 95$ %, the value of the expanded uncertainty of BP measurements was calculated using the formula [29]–[34]:

$$U = \frac{k_p\, \tilde{u}_c\, \overline{BP}}{100\ \%}. \tag{15}$$

Substituting the obtained maximum values of the experimental uncertainty of BP measurements into formula (15), it was found that the expanded uncertainty of SBP measurements was ± 11.55 mmHg, and the expanded uncertainty of DBP measurements does not exceed ± 7.84 mmHg at a confidence level of 95 %.

Thus, the results of the BP studies of patient 1 can be presented as:

$\overline{SBP} = 113 \pm 11.55$ mmHg at p = 95 %,

$\overline{DBP} = 83.4 \pm 7.84$ mmHg at p = 95 %,

and for patient 2:

$\overline{SBP} = 112.12 \pm 11.55$ mmHg at p = 95 %,

$\overline{DBP} = 84 \pm 7.84$ mmHg at p = 95 %.

The findings indicate that Method 3 (Subsection 3.2.3), which applies model (3) for estimating SBP and model (9) for calculating DBP based on the reference MBP value defined by equation (8), yields the most accurate BP measurements.

Thus, the proposed mathematical models for calculating SBP and DBP, along with the methodology for evaluating measurement uncertainty - which accounts for both Type A evaluation of uncertainty and Type B evaluation of uncertainty associated with the limited accuracy of the measurement equipment - were validated experimentally. The results confirmed the feasibility of BP estimation with expanded uncertainties of ± 11.55 mmHg for SBP and ± 7.84 mmHg for DBP at a 95% confidence level. The obtained values of expanded measurement uncertainty comply with the Grade A accuracy category defined by the British Hypertension Society, which states that, at a 95% confidence level, the deviations in SBP and DBP measurements should not exceed ± 15 mmHg.

5. CONCLUSIONS

Considering the specifics of using the MAX86150 Evaluation System for measuring ECG and PPG signals, our team developed mathematical models for the indirect estimation of SBP and DBP using fingertip measurements. These models were tested in the MATLAB environment. A database of ECG and PPG signals was collected from two patients, aged 42 and 66 years. Using the proposed mathematical models, the signals were processed in MATLAB, and the results of the indirect BP measurements were presented in Table 1 and Table 2.

The algorithm for BP estimation based on mathematical models (3) and (9) demonstrated the highest accuracy. In this approach, DBP was determined based on the MBP. The expanded uncertainty of BP measurements was ± 11.55 mmHg for SBP and ± 7.84 mmHg for DBP at a confidence level of 95 %, which meets the clinical accuracy requirements set by the British Hypertension Society (BHS) and the AAMI/ANSI/ISO 81060-2:2018 standard.

However, it should be noted that the study was limited using only two patients, which restricts the generalizability of the findings. This limitation should be addressed in future studies involving larger and more diverse populations to confirm the robustness of the proposed methodology. Future research will focus on expanding the dataset and comparing the indirect SBP and DBP estimates with reference BP values measured using a high-precision cuff-based device. Based on this comparison, a method for incorporating correction factors into the estimation algorithm will be developed to improve reliability and clinical applicability.

REFERENCES

[1] P. C.-P. Chao, C.-C. Wu, D. H. Nguyen, B.-S. Nguyen, P.-C. Huang, V.-H. Le, The Machine Learnings Leading the Cuffless PPG Blood Pressure Sensors Into the Next Stage, IEEE Sensors Journal, vol. 21, no. 11, pp. 12498–12510, 2021. DOI: 10.1109/jsen.2021.3073850

[2] J. Yan, Z. Wang, R. Guo, H. Yan, Y. Wang, W. Qiu, Blood pressure prediction based on multi-sensor information fusion of electrocardiogram, photoplethysmography, and pressure pulse waveform, Measurement, Volume 240, 2025, 115446. DOI: 10.1016/j.measurement.2024.115446

[3] B. Tóth, D. Senti, T. Mar Ingolfsson, J. Zweidler, A. Elsig, L. Benini, Y. Li, Finetuning and Quantization of EEG-Based Foundational BioSignal Models on ECG and PPG Data for Blood Pressure Estimation, Signal Processing, 2025, arXiv preprint arXiv:2502.17460. DOI: 10.48550/arXiv.2502.17460

[4] P.-K. Man, K.-L. Cheung, N. Sangsiri, W.J. Shek, K.-L. Wong, J.-W. Chin, T.-T. Chan, R.H.-Y. So, Blood Pressure Measurement: From Cuff-Based to Contactless Monitoring, Healthcare, vol. 10, 10, 2022, p. 2113. DOI: 10.3390/healthcare10102113

[5] H. Samimi, H. Dajani, Cuffless Blood Pressure Estimation Using Calibrated Cardiovascular Dynamics in the Photoplethysmogram, Bioengineering, vol. 9, no. 9, 2022, p. 446. DOI: 10.3390/bioengineering9090446

[6] M. Sharma, K. Barbosa, V. Ho, D. Griggs, T. Ghirmai, S. K. Krishnan, T. K. Hsiai, J.-C. Chiao, H. Cao,Cuff-Less and Continuous Blood Pressure Monitoring: A Methodological Review, Technologies, vol. 5, no. 2, 2017, p. 21. DOI: 10.3390/technologies5020021

[7] Thinklabs, Thinklabs Homepage, Online [Accessed 19 June 2025] https://www.thinklabs.com

[8] S. Gómez-Quintana, C. E. Schwarz, I. Shelevytsky, V. Shelevytska, O. Semenova, A. Factor, E. Popovici, A. Temko, A Framework for AI-Assisted Detection of Patent Ductus Arteriosus from Neonatal Phonocardiogram, Healthcare, 2021, 9, 169. DOI: 10.3390/healthcare9020169

[9] O. Vasilevskyi, E. Popovici, V. Sarana, Modeling and analysis of systolic and diastolic blood pressure using ECG and PPG signals, Informatyka, Automatyka, Pomiary W Gospodarce I Ochronie Środowiska, 2023, 13(3), pp. 5–10. DOI: 10.35784/iapgos.5326

[10] M. Kachuee, M. M. Kiani, H. Mohammadzade, M. Shabany, Cuffless Blood Pressure Estimation Algorithms for Continuous Health-Care Monitoring, in IEEE Transactions on Biomedical Engineering, 2017, 64, 4, 859-869. DOI: 10.1109/TBME.2016.2580904

[11] AnalogDevices, MAX86150 Evaluation System, Online [Accessed 19 June 2025] https://www.analog.com/media/en/technical-documentation/data-sheets/MAX86150EVSYS.pdf

[12] M. Pour Ebrahim, F. Heydari, T. Wu, K. Walker, K. Joe, J.-M. Redoute, M. Rasit Yuce, Blood Pressure Estimation Using On-body Continuous Wave Radar and Photoplethysmogram in Various Posture and Exercise Conditions, Sci Rep 9, 2019, 16346. DOI: 10.1038/s41598-019-52710-8

[13] G. Fortino, V. Giampà, PPG-based methods for non invasive and continuous blood pressure measurement: an overview and development issues in body sensor networks, 2010 IEEE Int. Workshop on Medical Measurements and Applications, Ottawa, ON, Canada, 30 April 2010 - 1 May 2010, pp. 10-13. DOI: 10.1109/MEMEA.2010.5480201

[14] Q. Zhang, X. Zeng, W. Hu, D. Zhou, A Machine Learning-Empowered System for Long-Term Motion-Tolerant Wearable Monitoring of Blood Pressure and Heart Rate With Ear-ECG/PPG, in IEEE Access, 2017, vol. 5, pp. 10547-10561. DOI: 10.1109/ACCESS.2017.2707472

[15] R. Mukkamala, J.-O. Hahn, O. T. Inan, L. K. Mestha, C.-S. Kim, H. Töreyin, S. Kyal, Toward Ubiquitous Blood Pressure Monitoring via Pulse Transit Time: Theory and Practice, in IEEE Transactions on Biomedical Engineering, 62, 8, 2015, pp. 1879-1901. DOI: 10.1109/TBME.2015.2441951

[16] Y. C. Chiu, P. W. Arand, S. G. Shroff, T. Feldman, John D. Carroll, Determination of pulse wave velocities with computerized

algorithms, American Heart Journal, 1991, Volume 121, Issue 5, pp. 1460-1470.
DOI: 10.1016/0002-8703(91)90153-9

[17] R. A. Payne, C. N. Symeonides, D. J. Webb, S. R. J. Maxwell, Pulse transit time measured from the ECG: an unreliable marker of beat-to-beat blood pressure, Journal of Applied Physiology, 2006, 100(1), pp. 136-141.
DOI: 10.1152/japplphysiol.00657.2005

[18] American Heart Association, Understanding Blood Pressure Readings. Online [Accessed 19 June 2025] https://www.heart.org/en/health-topics/high-blood-pressure/understanding-blood-pressure-readings

[19] C. A. Haque, T.-H. Kwon, K.-D. Kim, Cuffless Blood Pressure Estimation Based on Monte Carlo Simulation Using Photoplethysmography Signals, Sensors, 2022, 22, 1175.
DOI: 10.3390/s22031175

[20] Y.-H. Kao, P. C.-P. Chao, C. -L. Wey, Design and Validation of a New PPG Module to Acquire High-Quality Physiological Signals for High-Accuracy Biomedical Sensing, in IEEE Journal of Selected Topics in Quantum Electronics, 2019, vol. 25, 1, pp. 1-10.
DOI: 10.1109/JSTQE.2018.2871604

[21] J. H.-S. Wang, M.-H. Yeh, P. C.-P. Chao, T.-Y. Tu, Y.-H. Kao, R. Pandey, A fast digital chip implementing a real-time noise-resistant algorithm for estimating blood pressure using a non-invasive, cuffless PPG sensor, Microsyst Technol, 2020, 26, 3501–3516.
DOI: 10.1007/s00542-020-04946-y

[22] C.-H. Tseng, T.-J. Tseng, C.-Z. Wu, Cuffless Blood Pressure Measurement Using a Microwave Near-Field Self-Injection-Locked Wrist Pulse Sensor, in IEEE Transactions on Microwave Theory and Techniques, 2020, vol. 68, no. 11, pp. 4865-4874.
DOI: 10.1109/TMTT.2020.3011446

[23] Q. J. Xiao, Zh. Luo, J. Wu, Study on Wavelet Packet Denoising Technique and its Application in Mechanical Fault Diagnosis, Applied Mechanics and Materials, 2015, vol. 713–715, pp. 445–448.
DOI: www.scientific.net/amm.713-715.445

[24] H. Wu, Z. Ji, M. Li, Non-Invasive Continuous Blood-Pressure Monitoring Models Based on Photoplethysmography and Electrocardiography, Sensors, 2019, 19, 5543.
DOI: 10.3390/s19245543

[25] JCGM 100:2008. Evaluation of measurement data — Guide to the expression of uncertainty in measurement. Joint Committee for Guides in Metrology (JCGM), 2008.

[26] O. Vasilevskyi, Assessing the level of confidence for expressing extended uncertainty through control errors on the example of a model of a means of measuring ion activity, Acta IMEKO, vol. 10, no. 2, article 27, 2021, pp. 199-203.
DOI: 10.21014/acta_imeko.v10i2.810

[27] R. Trishch, O. Maletska, H. Hrinchenko, S. Artiukh, V. Burdeina, N. Antonenko, Development and validation of measurement techniques according to ISO/IEC 17025:2017, 2019 IEEE 8th International Conference on Advanced Optoelectronics and Lasers (CAOL), 2019, pp. 1–6.
DOI: 10.1109/caol46282.2019.9019539

[28] O. Vasilevskyi, M. Koval, S. Kravets, Indicators of reproducibility and suitability for assessing the quality of production services, Acta IMEKO, vol. 10, no. 4, article 11, 2021, pp. 54-61.
DOI: 10.21014/acta_imeko.v10i4.814

[29] O. M. Vasilevskyi, P. Kulakov, I. A. Dudatiev, V. M. Didych, (+ another 4 authors), Vibration diagnostic system for evaluation of state interconnected electrical motors mechanical parameters, Photonics Applications in Astronomy, Communications, Industry, and High Energy Physics Experiments 2017, vol. 10445, 2017, p. 104456C.
DOI: 10.1117/12.2280993

[30] A. Semenov, O. Osadchuk, O. Semenova, O. Bisikalo, O. Vasilevskyi, O. Voznyak, Signal Statistic and Informational Parameters of Deterministic Chaos Transistor Oscillators for Infocommunication Systems, 2018 Int. Scientific-Practical Conf. Problems of Infocommunications. Science and Technology, Kharkiv, Ukraine, 9-12 October 2018, pp. 730–734.
DOI: 10.1109/infocommst.2018.8632046

[31] M. Riabchykov et al., Prospects for the Development of Smart Clothing with the Use of Textile Materials with Magnetic Properties, Tekstilec, vol. 65, no. 1, 2022, pp. 36–43.
DOI: 10.14502/tekstilec.65.2021050

[32] O. Vasilevskyi, V. M. Sevastianov, K. V. Ovchynnykov, V. M. Didych, S. A. Burlaka, Accuracy of Potentiometric Methods for Measuring Ion Activity in Solutions, Proceedings of Seventh International Congress on Information and Communication Technology, 2022, pp. 181–189.
DOI: 10.1007/978-981-19-1607-6_16

[33] O. Kupriyanov, R. Trishch, D. Dichev, K. Kupriianova, A General Approach for Tolerance Control in Quality Assessment for Technology Quality Analysis, Lecture Notes in Mechanical Engineering, 2023, pp. 330–339.
DOI: 10.1007/978-3-031-16651-8_31

[34] O. Vasilevskyi, O. Voznyak, V. Didych, V. Sevastianov, O. Ruchka, V. Rykun, Methods for Constructing High-precision Potentiometric Measuring Instruments of Ion Activity, 2022 IEEE 41st Int. Conf. on Electronics and Nanotechnology (ELNANO), Kyiv, Ukraine, 10-14 October 2022, pp. 247-252.
DOI: 10.1109/ELNANO54667.2022.9927128